EPB41L4A-AS1 promotes endothelial dysfunction in preeclampsia through the miR-26a-2-3p/15-LOX-1/p38 MAPK axis

JUNGONG HE[1*], HONGXU RAN[1*], RONGSONG XIA[2], ZHE PENG[3], YAN LIU[4], XIAOYI CHENG[2], YIBEI ZHAO[5], DONGZHI RAN[1], LIN CHEN[3] and JUNQING YANG[1,3]

[1]Chongqing Key Laboratory of Biochemistry and Molecular Pharmacology, Chongqing Medical University, Chongqing 400016, P.R. China; [2]Department of Pharmacy, Chongqing General Hospital, Chongqing University, Chongqing 401147, P.R. China; [3]Department of Pharmacy, Women and Children's Hospital of Chongqing Medical University, Chongqing 400013, P.R. China; [4]Department of Pharmacy, Guizhou Branch of Shanghai Children's Medical Center, Shanghai Jiao Tong University School of Medicine, Guiyang, Guizhou 550081, P.R. China; [5]Department of Histology and Embryology, Third Military Medical University (Army Medical University), Chongqing 400038, P.R. China

Received November 5, 2025; Accepted October 6, 2026

DOI: 10.3892/ijmm.2026.6059

Abstract. Preeclampsia (PE) is a hypertensive disorder of pregnancy characterized by systemic endothelial dysfunction. Long non-coding RNA EPB41L4A-AS1 has been implicated in pregnancy-related disorders, but its role in PE remains unclear. Our previous work demonstrated that downregulation of miR-26a-2-3p promotes endothelial injury via activation of the 15-lipoxygenase-1 (15-LOX-1)/p38 mitogen-activated protein kinase (p38 MAPK) pathway. In the present study, whether EPB41L4A-AS1 contributes to PE pathogenesis by regulating this axis was investigated. EPB41L4A-AS1 expression was significantly upregulated in placental tissues from patients with PE and negatively correlated with miR-26a-2-3p levels. Functional experiments revealed that EPB41L4A-AS1 overexpression suppressed miR-26a-2-3p, activated the 15-LOX-1/p38 MAPK pathway and promoted endothelial dysfunction, effects that were partially reversed by miR-26a-2-3p mimics. In an L-NAME-induced PE mouse model, EPB41L4A-AS1 overexpression exacerbated hypertension, proteinuria, placental apoptosis and oxidative stress, whereas miR-26a-2-3p agomir administration attenuated these effects. Mechanistically, luciferase reporter assays revealed no direct binding between EPB41L4A-AS1 and miR-26a-2-3p, suggesting an indirect regulatory mechanism. Collectively, these findings identify EPB41L4A-AS1 as a critical upstream regulator of the miR-26a-2-3p/15-LOX-1/p38 MAPK axis in PE and suggest that targeting this pathway may represent a potential therapeutic strategy.

Correspondence to: Dr Lin Chen, Department of Pharmacy, Women and Children's Hospital of Chongqing Medical University, 120 Longshan Road, Yubei, Chongqing 400013, P.R. China
E-mail: clfxmm@163.com

Dr Junqing Yang, Chongqing Key Laboratory of Biochemistry and Molecular Pharmacology, Chongqing Medical University, 1 Yixueyuan road, Yuzhong, Chongqing 400016, P.R. China
E-mail: cqyangjq@cqmu.edu.cn

*Contributed equally

Key words: preeclampsia, endothelial dysfunction, long non-coding RNA EPB41L4A-AS1, miR-26a-2-3p, apoptosis

Introduction

Preeclampsia (PE) is a pregnancy-specific syndrome marked by hypertension, proteinuria and various organ dysfunctions occurring at or after 20 weeks of gestation (1). It affects 2-8% of pregnancies worldwide and stands as the primary reason for maternal and perinatal morbidity and mortality (2). The pathogenesis of PE remains incompletely elucidated. It involves oxidative stress, inflammatory responses and metabolic disorders, among other factors, and results from the combined action of multiple mechanisms (3-5). Currently, there is no established cure other than ending the pregnancy (6); therefore, studying the pathogenesis and development mechanisms of PE is extremely crucial to maternal and fetal health.

A substantial body of literature elucidates that the two-stage process can clarify the pathogenesis of PE (7-9). Shallow trophoblast implantation and insufficient spiral artery remodeling lead to placental hypoxia and stress, which leads to the secretion of circulating factors, such as the anti-angiogenic factors soluble fms-like tyrosine kinase-1 (sFlt-1) and soluble endoglin (sEng), as well as the endothelial adhesion molecules soluble vascular cell adhesion molecule-1 (sVCAM-1) and soluble intercellular adhesion molecule-1 (sICAM-1). These factors collectively contribute to maternal endothelial dysfunction (10,11). Understanding the mechanisms of endothelial dysfunction is crucial for advancing the treatment of PE (12). Further exploration of these mechanisms can enhance the theoretical foundation for enhancing clinical management of PE.

MicroRNAs (miRNAs) are short non-coding RNAs of ~22 nucleotides that function as post-transcriptional gene regulators. By binding to target mRNA 3' untranslated regions, they

control key cellular events such as proliferation, differentiation, apoptosis and metabolism (13-15). Accumulating evidence implicates aberrant miRNA expression in various diseases, such as PE (16,17). For instance, the miRNAs miR-29a/c-3p, miR-31-5p, miR-155-5p, miR-214-3p and miR-1270 have been suggested to contribute to regulating endothelial cellular functions in PE (18-22). We previously demonstrated that in both patients with PE and mouse models, reduced placental miR-26a-2-3p leads to the upregulation of 15-lipoxygenase-1 (15-LOX-1). This upregulation promotes endothelial injury via p38 mitogen-activated protein kinase (p38 MAPK), thereby exacerbating disease progression (23). Nevertheless, the factors responsible for miR-26a-2-3p downregulation in PE are poorly defined. Therefore. The present study sought to explore the upstream regulatory events controlling its expression.

By binding to miRNAs, long noncoding RNAs (lncRNAs) regulate the expression of target genes and subsequently participate in a wide range of physiological functions (24). Over the years, considerable attention has been directed towards the role of competing endogenous RNA crosstalk in the pathological progression of PE (25). Consequently, the present study was particularly interested in investigating whether the downregulation of miR-26a-2-3p expression in placentas affected by PE is associated with the regulation of lncRNAs. The upstream lncRNAs of miR-26a-2-3p were predicted through the Targetscan website, among which EPB41L4A-AS1 exhibited potential binding sites with miR-26a-2-3p. Emerging evidence links aberrant EPB41L4A-AS1 expression to early recurrent miscarriage (26). Furthermore, a case-control study identified an association between its expression levels and neonatal birthweight (27). However, it is still unclear whether EPB41L4A-AS1 contributes to PE and if so, whether it acts through regulating miR-26a-2-3p to induce endothelial dysfunction.

The present investigation into the role of EPB41L4A-AS1 in PE revealed its significant upregulation in diseased placental tissues. Functional experiments confirmed that EPB41L4A-AS1 overexpression impaired endothelial function in both *in vivo* and *in vitro*. To determine if EPB41L4A-AS1 interacts with miR-26a-2-3p, their correlation and the comprehensive role of the EPB41L4A-AS1/miR-26a-2-3p/15-LOX-1/p38 MAPK pathway in endothelial dysfunction was analyzed. These findings provide insights with potential therapeutic implications for PE.

Materials and methods

Participants. Participants meeting the eligibility criteria were recruited from the Women and Children Hospital affiliated with Chongqing Medical University (Chongqing, China) between September 2020 and August 2022. A total of 45 pregnant women were included in the present study. Among them, 30 were diagnosed with preeclampsia (PE), with an age range of 21 to 49 years (median 31 years), and 15 were gestational age-matched healthy controls, with an age range of 27 to 34 years (median 31 years) (Table I). The inclusion criteria were as follows: i) Singleton pregnancy; ii) gestational age ≥20 weeks at delivery; iii) delivery by elective cesarean section; iv) for the PE group, diagnosis of PE according to the criteria described in a previous publication (23); v) for the control group, normal pregnancy without hypertension, proteinuria or other pregnancy-related complications; and vi) availability of complete clinical data and signed informed consent. The exclusion criteria were as follows: i) Multiple gestation; ii) chronic hypertension, pre-gestational diabetes mellitus, renal disease, autoimmune disease, cardiovascular disease or other severe maternal comorbidities; iii) fetal chromosomal abnormalities or major congenital malformations; iv) placental abnormalities such as placenta previa or placental abruption; v) active infection; vi) smoking, alcohol or drug abuse; and vii) incomplete clinical or placental data. The diagnostic criteria for PE were adopted from a previous publication (23). Ethical approval for this study was obtained from the Ethics Committee of the Women and Children's Hospital affiliated with Chongqing Medical University (approval no. SYXK YU 2022-0016, 2022033), and all patients provided signed informed consent.

Human placenta collection. Placental tissue was collected immediately following elective cesarean section. The collected tissues were rinsed twice in pre-cooled 0.9% normal saline to eliminate blood clots. Subsequently, the tissues were sub-packaged: A portion was rapidly frozen in liquid nitrogen and then transferred to an environment maintained at -80˚C for preservation, while the remaining portion was immersed in 4% paraformaldehyde solution and fixed at 4˚C overnight (~24 h). Patient clinical data were retrospectively collected from medical records. All diagnoses adhered to the criteria established by the American Board of Obstetrics and Gynecology (28).

Cell cultures and hypoxic treatment. Human umbilical vein endothelial cells (HUVECs) were cultured in complete growth medium consisting of RPMI-1640 (cat. no. 11875-093; Gibco; Thermo Fisher Scientific, Inc.) supplemented with 10% fetal bovine serum (cat. no. 10099141; Thermo Fisher Scientific, Inc.) and 1% penicillin/streptomycin (cat. no. C0222; Beyotime Biotechnology). Cells were maintained at 37˚C in a humidified atmosphere of 5% CO_2. Hypoxic treatments were performed as previously detailed (18). Briefly, HUVECs were maintained in a hypoxic chamber (1% O_2, 5% CO_2, and balance N_2) for 24 h, after which both conditioned supernatants and cells were subsequently collected for analysis.

Cell transfection. Following the manufacturer's instructions, both lncRNA and microRNA were delivered into HUVECs using Lipofectamine 3000 transfection reagent (cat. no. L3000008; Thermo Fisher Scientific, Inc.). The overexpression of EPB41L4A-AS1 and miR-26a-2-3p were performed using EPB41L4A-AS1 adenovirus (Shanghai GeneChem Co., Ltd.) and miR-26a-2-3p mimics (Sangon Biotech Co., Ltd.), The sequences of the miR-26a-2-3p mimics were derived from our previously published article and have been validated in the same HUVEC cell line (23). The sequences of the negative control (NC) for the miR-26a-2-3p mimics are as follows: The sense strand is 5'-UUGUACUACACAAAAGUACUG-3', and the antisense strand is 5'-GUACUUUUGUGUAGUACA AUU-3' (Sangon Biotech Co., Ltd.). For comparison, HUVECs transfected with NC adenovirus served as a negative control. Transfected cells were cultured at 37˚C under a humidified

Table I. Clinical characteristics of preeclamptic and normal pregnancies.

Characteristics	Normal group (n=15)	PE group (n=30)	P-value
Age, years	31.27±2.99	31.57±5.71	>0.05
Height, cm	158.87±5.24	162.20±17.31	>0.05
Weight, kg	67.57±8.64	72.33±12.72	>0.05
BMI, kg/m^2	26.49±2.45	27.99±5.62	>0.05
Systolic blood pressure, mmHg	112.80±12.07	158.40±17.31	<0.01
Diastolic blood pressure, mmHg	70.00±6.00	98.60±14.01	<0.01
Gestation days	271.67±9.78	252.37±20.11	<0.01
Proportion of initial pregnancies, %	26.67	60.00	<0.05
Urinary protein, g/24 h	0	3.88±4.22	<0.001
Fetal weight, g	3,344.67±375.73	2,475.17±785.57	<0.01

PE, preeclampsia.

5% CO_2 atmosphere for 24 h and then harvested for subsequent analyses.

Animal experiments. C57BL/6 mice (female mice, n=20; male mice, n=10; all 8-10 weeks old, median age of 9 weeks) were originally purchased from the Experimental Animal Center of Chongqing Medical University (Chongqing, China) [production license no. SCXK (Yu) 2022-0010] and were maintained under specific pathogen-free conditions at the same facility. All animals were maintained under specific pathogen-free conditions with a 12/12-h light/dark cycle, controlled temperature of 22±2˚C and relative humidity of 55-65%, with free access to food and water. Mating was established by housing females with weight-matched male mice overnight at a 2:1 ratio. The observation of a vaginal plug the following morning was defined as gestational day (GD 0.5). L-NAME (cat. no. S2877; Selleck Chemicals) was employed to establish a PE mouse model following established protocols (29). Subsequently, the pregnant animals were assigned to one of five groups at random: Control group, normal saline was given intragastrically from GD 12.5 to GD 18.5; PE group, 75 mg/kg L-NAME solution was given intragastrically from day GD 12.5 to GD 18.5; PE+Ad-NC group, 75 mg/kg L-NAME solution was given intragastrically from GD 12.5 to GD 18.5, and the corresponding amount of normal saline was injected into abdominal cavity at the same time; PE+Ad-EPB-AS1 group, 75 mg/kg L-NAME solution was given intragastrically from GD 12.5 to GD 18.5, and 5x10^8 PFU EPB41L4A-AS1 adenovirus was injected intraperitoneally on GD 12.5, GD 14.5 and GD 16.5; PE+Ad-EPB-AS1+agomir group, 75 mg/kg L-NAME solution was intragastrically administered from GD 12.5 to GD 18.5, and 5x10^8 PFU EPB41L4A-AS1 adenovirus and 5 μl 50 μM miR-26a-2-3p agomir solution were injected intraperitoneally on GD 12.5, GD 14.5 and GD 16.5.

On GD 12.5 and GD 18.5, systolic blood pressure in pregnant mice was assessed using a volume pressure-recording tail-cuff apparatus (VisiTech International). On GD 18.5, following euthanasia by pentobarbital anesthesia (150 mg/kg; cat. no. P3761; MilliporeSigma), maternal placenta, fetuses, urine and plasma samples were collected for subsequent analysis. Fetal and placental weights were documented. Urine protein levels were assessed using the Urine Protein Content Assay Kit (cat. no. BC5655; Beijing Solarbio Science & Technology Co., Ltd.) following the provided protocols. All animal experimental procedures were in compliance with the Ethical Committee for Animal Experimentation at Chongqing Medical University (approval no. SYXK-2022-0016). During the experimental period, animals exhibiting severe weight loss, lethargy, inability to eat or drink, labored breathing or persistent abnormal posture would be immediately euthanized under anesthesia with an overdose of pentobarbital (150 mg/kg, intraperitoneal injection) as a humane endpoint if any of these signs were observed prior to the scheduled experimental endpoint.

Western blot analysis. Cellular proteins were isolated with RIPA buffer (cat. no. P0013B; Beyotime Biotechnology) containing a cocktail of PMSF (cat. no. ST506; Beyotime Biotechnology), phosphatase (cat. no. P1082; Beyotime Biotechnology) and protease inhibitors (cat. no. P1005; Beyotime Biotechnology), and quantified by BCA assay (cat. no. P0012; Beyotime Biotechnology). Following quantification by BCA assay, equal amounts of protein (20 μg per lane) were separated on 10-12.5% SDS-PAGE gels and transferred to PVDF membranes (cat. no. IPVH00010; MilliporeSigma). Following blocking with 5% skim milk (cat. no. P0216; Beyotime Biotechnology) for 1 h at 37˚C, the membranes were probed with specific primary antibodies, including anti-15-LOX-1 (1:1,000; cat. no. ab244205; Abcam), anti-p38 MAPK (1:1,000; cat. no. 14064-1-AP; Proteintech Group, Inc.), anti-phospho-p38 MAPK (1:1,000; cat. no. 28796-1-AP; Proteintech Group, Inc.), anti-Bax (1:1,000; cat. no. 50599-2-Ig; Proteintech Group, Inc.) and anti-Bcl-2 (1:1,000; cat. no. 12789-1-AP; Proteintech Group, Inc.) at 4˚C overnight. β-actin (1:3,000; cat. no. 66009-1-Ig; Proteintech Group, Inc.) was used as the internal reference. After washing with Tris-buffered saline containing 0.01% (v/v) Tween-20, the membranes were treated with appropriate HRP-linked secondary antibodies (both at 1:1,000; anti-mouse: cat. no. ab6789; anti-rabbit: cat. no. ab6721; Abcam) for 1 h at 37˚C. Protein bands were then exposed with an ECL substrate

Table II. Quantitative PCR primers sequences.

Gene	Sequences
hsa-lncRNA-EPB41L4A-AS1 forward	5'-GCCTGGTTTTATTTTCGTCAGT-3'
hsa-lncRNA-EPB41L4A-AS1 reverse	5'-GCATCCATCTTCCACCTGTAG-3'
hsa-miR-26a-2-3p forward	5'-GCGCGCCTATTCTTGATTACT-3'
hsa-miR-26a-2-3p reverse	5'-AGTGCAGGGTCCGAGGTATT-3'
hsa-β-actin forward	5'-TGGCACCCAGCACAATGAA-3'
hsa-β-actin reverse	5'-CTAAGTCATAGTCCGCCTAGAAGCA-3'
U6 forward	5'-GGAACGATACAGAGAAGATTAGC-3'
U6 reverse	5'-TGGAACGCTTCACGAATTTGCG-3'
miR-26a-2-3p RT	5'-GTCGTATCCAGTGCAGGGTCCGAGG TATTCGCACTGGATACGACGAAACA-3'

(cat. no. BL520A; Biosharp Life Sciences) and captured by a ChemiDoc XRS+ system (Bio-Rad Laboratories, Inc.).

RNA extraction and reverse transcription-quantitative PCR (RT-qPCR). Total RNA was extracted from placental tissues or HUVECs using Trizol reagent (cat. no. 15596026; Invitrogen; Thermo Fisher Scientific, Inc.). Subsequently, cDNA synthesis was carried out with a PrimeScript RT reagent kit (cat. no. RR037A; Takara Bio, Inc.) in a 20 μl reaction system at 37˚C for 15 min, followed by inactivation at 85˚C for 5 sec. For qPCR, 20 ng of cDNA was amplified using the 2X SYBR Green Premix Pro Taq HS qPCR Kit (cat. no. AG11701; Accurate Biology; Hunan Aikerui Biotechnology Co., Ltd.) with 500 nM of each primer on a MyiQ Real-Time PCR Detection System (Bio-Rad Laboratories, Inc.). The amplification protocol consisted of 40 cycles under the following conditions: Denaturation at 95˚C for 30 sec, followed by 5 sec at 95˚C and 30 sec at 60˚C. The primers used are listed in Table II. The corresponding expression levels of EPB41L4A-AS1 and miR-26a-2-3p were normalized against the expression of β-actin or U6, and the data were processed using the comparative $2^{-\Delta\Delta Cq}$ method (30).

Hematoxylin and eosin (H&E) staining. Following overnight fixation in 4% paraformaldehyde at 4˚C, human placental tissues were processed through dehydration, paraffin-embedding and sectioning at 4 μm thickness. Sections were deparaffinized, rehydrated and stained with hematoxylin at room temperature for 5 min, followed by differentiation and bluing. After rinsing, the sections were counterstained with eosin at room temperature for 1 min. The stained sections were then dehydrated, cleared and mounted. Morphological features were examined under a light microscope (Olympus BX53; Olympus Corporation). Nuclei appeared blue and the cytoplasm appeared red.

Enzyme-linked immunosorbent assay (ELISA). Placental levels of 15-LOX-1, sFlt-1, sENG, sVCAM-1 and sICAM-1 were measured with specific ELISA kits (cat. no. UP-15LOX-1; cat. no. UP-sFlt1; cat. no. UP-sENG; cat. no. UP-sVCAM-1; cat. no. UP-sICAM-1; Hangzhou Zhenyoupin Biotechnology Co., Ltd.) according to the manufacturer's instructions.

TUNEL assay. Fixed human and mouse placental samples were routinely processed into 4 μm sections. After deparaffinization and rehydration, the sections were permeabilized with proteinase K at 37˚C for 20 min. The sections were then incubated with TUNEL reaction mixture (cat. no. C1088; Beyotime Biotechnology) at 37˚C for 60 min in the dark, followed by counterstaining with DAPI (cat. no. C1005; Beyotime Biotechnology) at room temperature for 10 min. Fluorescence images were captured using a fluorescence microscope (Olympus BX53; Olympus Corporation).

Flow cytometric analysis of cell apoptosis. The conditioned medium was removed, and the cells were rinsed twice with PBS. Subsequently, the cells were detached using EDTA-free trypsin to preserve membrane integrity for apoptosis detection. Cell apoptosis was assessed with an Annexin V-FITC/PI Apoptosis Detection Kit (cat. no. CA1020; Beijing Solarbio Science & Technology Co., Ltd.) according to the manufacturer's instructions and analyzed immediately on a CytoFLEX S flow cytometer (Beckman Coulter, Inc.) with CytExpert software (version 2.4; Beckman Coulter, Inc.) and FlowJo software (version 10.8.1; FlowJo, LLC). The cell populations were categorized into viable, necrotic, early apoptotic and late apoptotic groups, with the apoptotic cells (early + late) being used for further comparative analysis.

Cell Counting Kit-8 (CCK-8) assay. The viability of HUVECs was determined using a CCK-8 kit (cat. no. BS350B; Biosharp Life Sciences). An appropriate number of cells ($1x10^3$) suspended in a 100 μl complete medium were seeded into each well of a 96-well plate and mixed with 10 μl of CCK-8 reagent. After incubation at 37˚C for 1 h, the viability was measured at 450 nm using a microplate reader (Thermo Fisher Scientific, Inc.).

Cell migration assays. A Transwell assay was performed to evaluate HUVEC migration. Briefly, $5x10^4$ cells in 150 μl serum-free RPMI-1640 medium were seeded into the upper chamber, while the lower chamber contained 550 μl complete RPMI-1640 medium supplemented with 10% FBS as a chemoattractant. After incubation at 37˚C in a humidified atmosphere of 5% CO_2 for 24 h, non-migrated cells on

the upper membrane surface were removed. Cells that had migrated to the lower side were fixed with methanol at room temperature (~25˚C) for 30 min, stained with 0.1% crystal violet at room temperature for 30 min, and washed three times with PBS at room temperature. The number of migrated cells was counted under an optical microscope in three randomly selected fields.

Dual luciferase reporter assay. The potential binding sequence of EPB41L4A-AS1 and miR-26a-2-3p was predicted using TargetScanHuman Release 8.0 (https://www.targetscan.org/vert_80/). The binding sequence as well as its mutant sequence were inserted into the pGL3 vector (cat. no. E1751; Promega Corporation) to create the EPB41L4A-AS1-WT and EPB41L4A-AS1-MUT reporter vectors. Then mimics NC and miR-26a-2-3p mimics were, respectively, mixed with EPB41L4A-AS1-MUT and EPB41L4A-AS1-WT recombinant plasmids and were transfected into 293T cells through Lipo8000 transfection reagent (cat. no. C0533; Beyotime Biotechnology). After 24 h of transfection, luciferase activity was measured at 37˚C using the Dual-Luciferase Reporter Assay System (cat. no. E1910; Promega Corporation). Firefly luciferase activity was normalized to Renilla luciferase activity derived from the co-transfected pRL-TK plasmid (cat. no. E2241; Promega Corporation), and the relative luciferase activity was expressed as the firefly/Renilla ratio.

Immunofluorescence (IF) and fluorescence in situ hybridization (FISH). Following standard dewaxing, hydration and antigen retrieval procedures, 5 μm placental sections were probed with an anti-CD31 primary antibody (1:200; cat. no. GB12063; Wuhan Servicebio Technology Co., Ltd.) overnight at 4˚C, followed by incubation with an Alexa Fluor 488-conjugated goat anti-rabbit IgG (H+L) secondary antibody (1:500; cat. no. GB25301; Wuhan Servicebio Technology Co., Ltd.) at 37˚C for 1 h. For the subsequent FISH assay, EPB41L4A-AS1 was targeted with a set of eight single-stranded DNA oligonucleotide probes (24-28 nt), and miR-26a-2-3p was targeted with a single antisense single-stranded DNA probe (22 nt). All probes were designed against NCBI RefSeq NR_015370.2 (EPB41L4A-AS1) and miRBase MIMAT0004681 (hsa-miR-26a-2-3p), respectively, and were custom-synthesized by Servicebio (Wuhan Servicebio Technology Co., Ltd.) using the SweAMI ISH probe synthesis service (cat. no. GDP1087). EPB41L4A-AS1 signals were visualized in the Cy3 (red) channel, and miR-26a-2-3p signals were acquired in the far-red (Cy5) channel and are displayed in pink. Sections were prehybridized and then hybridized with the EPB41L4A-AS1 and miR-26a-2-3p probes at 75˚C, followed by stringency washes and sequential hybridization with SweAMI branch and signal probes according to the manufacturer's instructions. Because all probes were chemically synthesized, no plasmid template, *in vitro* transcription, PCR amplification or DNase digestion step was required. Cell nuclei were finally counterstained with DAPI (cat. no. C1005; Beyotime Biotechnology). Probe lengths and full sequences are provided in Table SI.

Bioinformatics. The binding sites between EPB41L4A-AS1 and miR-26a-2-3p were predicted through the Targetscan (http://www.targetscan.org/) website.

Superoxide dismutase (SOD) activity and malondialdehyde (MDA) content assay. SOD activity and MDA levels in placental samples were measured using dedicated assay kits (Superoxide Dismutase Activity Assay Kit, cat. no. BC5165; Malondialdehyde Content Assay Kit, cat. no. BC0020; both from Beijing Solarbio Science & Technology Co., Ltd.) according to the manufacturer's instructions.

Statistical analysis. All data analyses were conducted using GraphPad Prism software (version 8.0; Dotmatics). Data obtained from three independent replicates are presented as the mean ± SEM. Comparisons between two independent groups were performed using an unpaired two-tailed Student's t-test. Comparisons among three or more independent groups were performed using one-way ANOVA followed by Tukey's post hoc test. Correlations were analyzed by Spearman's rank-order correlation. $P<0.05$ was considered to indicate a statistically significant difference.

Results

Dysregulation of EPB41L4A-AS1 and miR-26a-2-3p/15-LOX-1/p38 MAPK axis in PE. Previous findings from our group have demonstrated that the miR-26a-2-3p/15-LOX-1/p38 MAPK signaling axis is instrumental in promoting endothelial cell injury in PE (18); however, its upstream regulatory mechanism remains unclear. Bioinformatics prediction revealed potential binding sites between miR-26a-2-3p and EPB41L4A-AS1 (Fig. S1A). To investigate the role of EPB41L4A-AS1 in the pathogenesis of PE and the association between EPB41L4A-AS1 and the miR-26a-2-3p/15-LOX-1/p38 MAPK axis in PE, placental tissues were collected. H&E staining identified key pathological features in PE placentas, including retroplacental hematoma and augmented intervillous fibrin, reflecting a state of maternal-fetal hypoperfusion (Fig. 1A). Additionally, compared with those frofm the normal pregnancy (NP) group, TUNEL assay demonstrated increased apoptosis in placentas from the PE group (Fig. 1B). RT-qPCR analysis demonstrated a significant increase in EPB41L4A-AS1 levels but a concurrent decrease in miR-26a-2-3p expression in PE placentas compared with the NP group (Fig. 1C and D). Accordingly, IF and FISH analysis also indicated higher EPB41L4A-AS1 expression and lower miR-26a-2-3p expression in PE placentas. Statistically, the levels of EPB41L4A-AS1 were negatively correlated with the levels of miR-26a-2-3p (Fig. 1E). Furthermore, both EPB41L4A-AS1 and miR-26a-2-3p were observed in the nuclear compartment of vascular endothelial cells, as identified by CD31 co-staining in IF and FISH assays (Fig. 1F). Consistent with our prior study, western blotting confirmed a significant induction of 15-LOX-1, p38 MAPK, phospho-p38 MAPK and Bax proteins in PE placentas, with a converse pattern observed for Bcl-2 (Fig. 1G). The converging evidence from the present study establishes a pathologic network involving EPB41L4A-AS1 and the miR-26a-2-3p/15-LOX-1/p38 MAPK axis in the pathophysiology of preeclampsia.

The placental tissue concentrations of sFlt-1, sENG, sVCAM-1 and sICAM-1 were measured. Analysis revealed a marked reduction in sVCAM-1 levels from PE placentas, while sICAM-1, sENG and sFlt-1 showed no significant

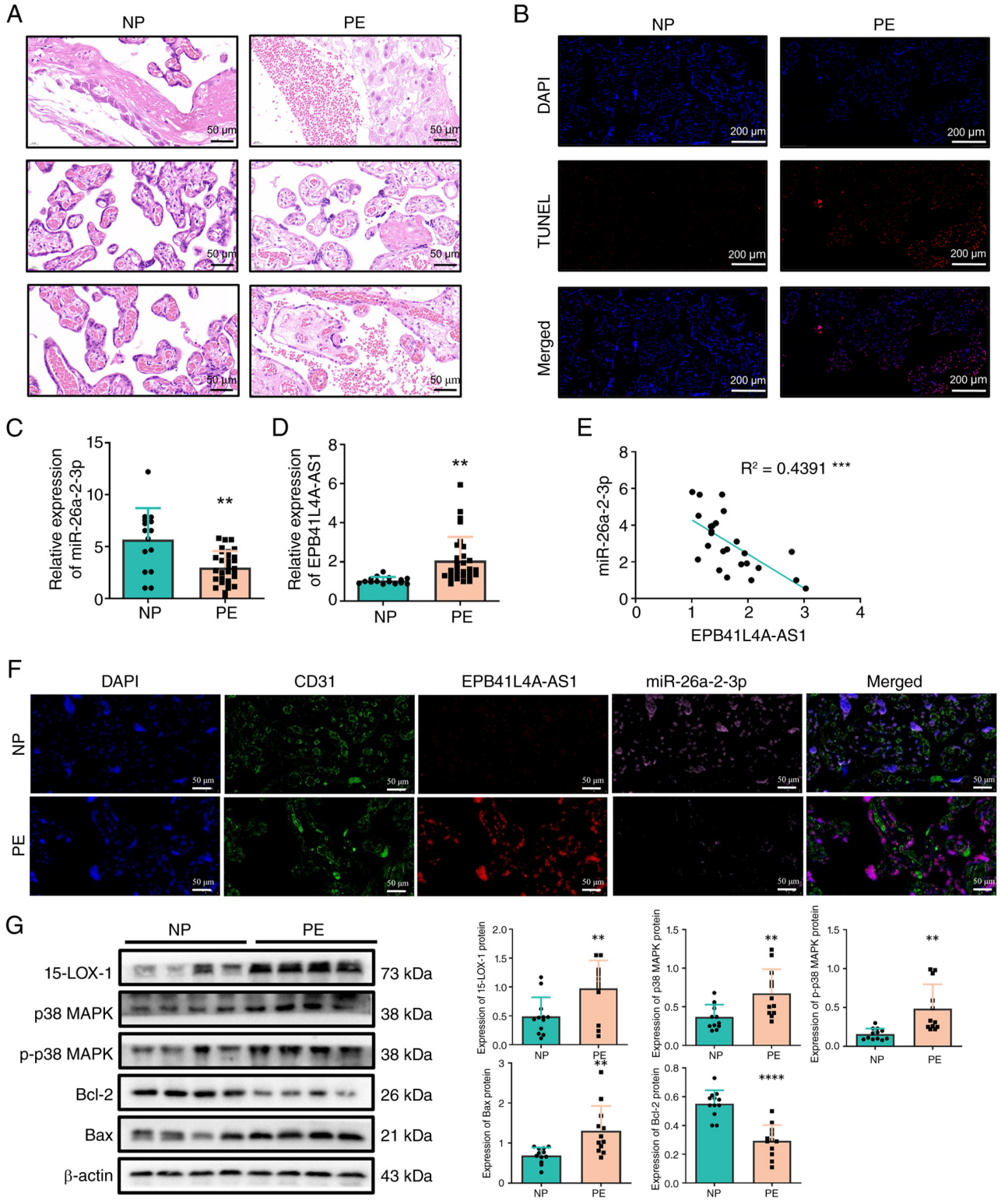


Figure 1. Dysregulation of EPB41L4A-AS1 and miR-26a-2-3p/15-LOX-1/p38 MAPK axis in PE. (A) H&E staining was used to detection the change of histopathology of the placenta in patients with PE. Scale bars, 50 μm. (B) TUNEL staining was used to observe apoptosis in placental tissue. DAPI (blue), TUNEL (red), scale bars, 200 μm. (C and D) The expression of miR-26a-2-3p and EPB41L4A-AS1 in placenta. (Control group: n=15, PE group: n=30). (E) Correlation analysis of EPB41L4A-AS1 and miR-26a-2-3p in placenta in patients with PE. (n=25). (F) Localization and expression of EPB41L4A-AS1 and miR-26a-2-3p in placenta in patients with preeclampsia. DAPI (blue), CD31 (green), EPB41L4A-AS1 (red), miR-26a-2-3p (pink), scale bars, 50 μm. (G) Relative protein expression of 15-LOX-1, p38 MAPK, phospho-p38 MAPK, Bax and Bcl-2 in placental. (Control group: n=12, PE group: n=12). **P<0.01, ***P<0.001 and ****P<0.0001. PE, preeclampsia; NP, normal pregnancy; 15-LOX-1, 15-lipoxygenase-1.

alterations (Fig. S2). This tissue-specific profile presents a striking contrast to our prior findings in the circulation, where sFlt-1, sICAM-1, and sVCAM-1 were all significantly elevated in patients with PE. This tissue-specific profile contrasts with our previous findings in the maternal circulation, where sFlt-1, sICAM-1 and sVCAM-1 were all

significantly elevated in patients with PE. This discrepancy is likely attributable to the different biological compartments examined: The placenta releases excessive amounts of these soluble factors into the maternal bloodstream, leading to elevated circulating levels, whereas the factors retained within placental tissue may be rapidly shed, locally bound or degraded, and thus may not show a corresponding increase in tissue homogenates.

EPB41L4A-AS1 regulates miR-26a-2-3p/15-LOX-1/p38 MAPK axis in HUVECs. The expression of EPB41L4A-AS1 was negatively correlated with miR-26a-2-3p in PE samples, which prompted the exploration of the association between EPB41L4A-AS1 and the miR-26a-2-3p/15-LOX-1/p38 MAPK axis *in vitro*. Following hypoxia exposure, the expression level of EPB41L4A-AS1 significantly increased, while that of miR-26a-2-3p significantly decreased (Fig. 2A and B). EPB41L4A-AS1 transfection was performed in HUVECs to investigate its potential regulatory effect on miR-26a-2-3p expression, with successful transfection confirmed in Fig. 2C and D. RT-qPCR data demonstrated that overexpression of EPB41L4A-AS1 reduced miR-26a-2-3p expression, whereas miR-26a-2-3p mimic reversed this change (Fig. 2E and F). Furthermore, IF and FISH assays were employed to examine the expression profiles and distribution of both molecules. As expected, EPB41L4A-AS1 and miR-26a-2-3p were exhibited precise co-localization within the nuclei of HUVECs. Under hypoxic conditions, a substantial upregulation of EPB41L4A-AS1 was observed, concurrently with a pronounced reduction in miR-26a-2-3p levels relative to the control group (Fig. 2G). To assess the potential interaction between EPB41L4A-AS1 and miR-26a-2-3p, luciferase reporter assays were performed. Results revealed no direct binding between these molecules (Fig. S1B), suggesting EPB41L4A-AS1 likely modulates miR-26a-2-3p expression through indirect mechanisms. Building upon our previous finding that miR-26a-2-3p modulates the 15-LOX-1/p38 MAPK pathway, Western blot analysis revealed that EPB41L4A-AS1 upregulation enhanced the expression of 15-LOX-1, p38 MAPK, phospho-p38 MAPK, and Bax, but suppressed Bcl-2. Notably, these effects were partially rescued by miR-26a-2-3p mimic co-transfection (Fig. 2H).

EPB41L4A-AS1 promoted the endothelial cells injury induced by hypoxia through miR-26a-2-3p/15-LOX-1/p38 MAPK axis in HUVECs. Meanwhile, the overexpression of EPB41L4A-AS1 significantly increased cell apoptosis (Fig. 3A), reduced endothelial cell viability (Fig. 3B) and migration capacity compared to the hypoxia group (Fig. 3C). Furthermore, ELISA analysis revealed markedly elevated concentrations of sFlt-1, sENG, sVCAM-1 and sICAM-1 in hypoxic HUVECs compared with the control group. The overexpression of EPB41L4A-AS1 further increased the levels of these factors in hypoxia-induced HUVECs (Fig. 3D). Moreover, miR-26a-2-3p mimic partially rescued the endothelial cells injury induced by the overexpression of EPB41L4A-AS1. Collectively, these results indicate that EPB41L4A-AS1 mediates hypoxic endothelial damage by potentiating apoptotic activity, reducing viability, impairing migration, and disrupting angiogenesis via the miR-26a-2-3p/15-LOX-1/p38-MAPK axis.

EPB41L4A-AS1 regulates miR-26a-2-3p/15-LOX-1/p38 MAPK axis in vivo. To delineate the *in vivo* regulatory network involving EPB41L4A-AS1, miR-26a-2-3p, 15-LOX-1 and p38 MAPK, further investigations were conducted using an L-NAME-induced murine PE model. As shown in Fig. 4A and B, mice transduced with Ad-EPB41L4A-AS1 exhibited robust overexpression of the target lncRNA compared with control groups. The placental levels of key molecules were examined in the PE-like mouse model, including 15-LOX-1, p38 MAPK, phospho-p38 MAPK, Bax, Bcl-2, and miR-26a-2-3p. RT-qPCR analysis indicated a significant downregulation of miR-26a-2-3p in the PE model group relative to controls. In parallel, western blotting demonstrated elevated protein expression of 15-LOX-1, p38 MAPK, phospho-p38 MAPK, and Bax, while Bcl-2 expression was concurrently reduced. EPB41L4A-AS1 overexpression significantly upregulated 15-LOX-1, p38 MAPK, phospho-p38 MAPK and Bax, while downregulating miR-26a-2-3p and Bcl-2. These alterations were partially rescued by miR-26a-2-3p mimic co-transfection (Fig. 4C and D). IF and FISH analyses revealed nuclear enrichment of both EPB41L4A-AS1 and miR-26a-2-3p in vascular endothelial cells. Furthermore, placental tissues from PE-model mice exhibited an inverse association between these molecules, with elevated EPB41L4A-AS1 and reduced miR-26a-2-3p (Fig. 4E).

EPB41L4A-AS1 activated 15-LOX-1/p38 MAPK axis to promote endothelial cell injury via mediating miR-26a-2-3p in PE-like mice. Next, the role of EPB41L4A-AS1/miR-26a-2-3p/15-LOX-1/p38 MAPK axis in PE was further investigated *in vivo*. TUNEL staining revealed increased apoptosis in the placenta of PE-like mice. EPB41L4A-AS1 significantly intensified this effect (Fig. 5A). Meanwhile, EPB41L4A-AS1 exacerbated the characteristic symptoms of PE in the L-NAME model, manifesting as heightened systolic hypertension and elevated urinary protein levels (Fig. 5B and C). Given the well-documented link between oxidative stress and endothelial damage in preeclampsia (7,10), the oxidative stress status was assessed in the mouse model by determining placental SOD activity and MDA content. Analysis revealed markedly reduced SOD activity along with considerably elevated MDA levels in PE-model mice compared to controls. EPB41L4A-AS1 aggravated the oxidative stress by inducing a significant decrease in SOD activity and a concomitant increase in MDA levels (Fig. 5D and E). Assessment by ELISA quantified significantly increased placental levels of sFlt-1, sENG, sVCAM-1 and sICAM-1 in the PE-like mouse. This dysregulation of angiogenesis and adhesion markers were further amplified by EPB41L4A-AS1 overexpression (Fig. 5F). Notably, administration of miR-26a-2-3p agomir partially alleviated the EPB41L4A-AS1-induced endothelial injury (Fig. 5A-F). In summary, the present findings demonstrate that EPB41L4A-AS1 upregulates the 15-LOX-1/p38 MAPK pathway by suppressing miR-26a-2-3p, thereby driving endothelial injury in the PE mouse model.

Discussion

As a severe obstetric syndrome, PE represents a major cause of maternal and perinatal morbidity and mortality (1). Currently,

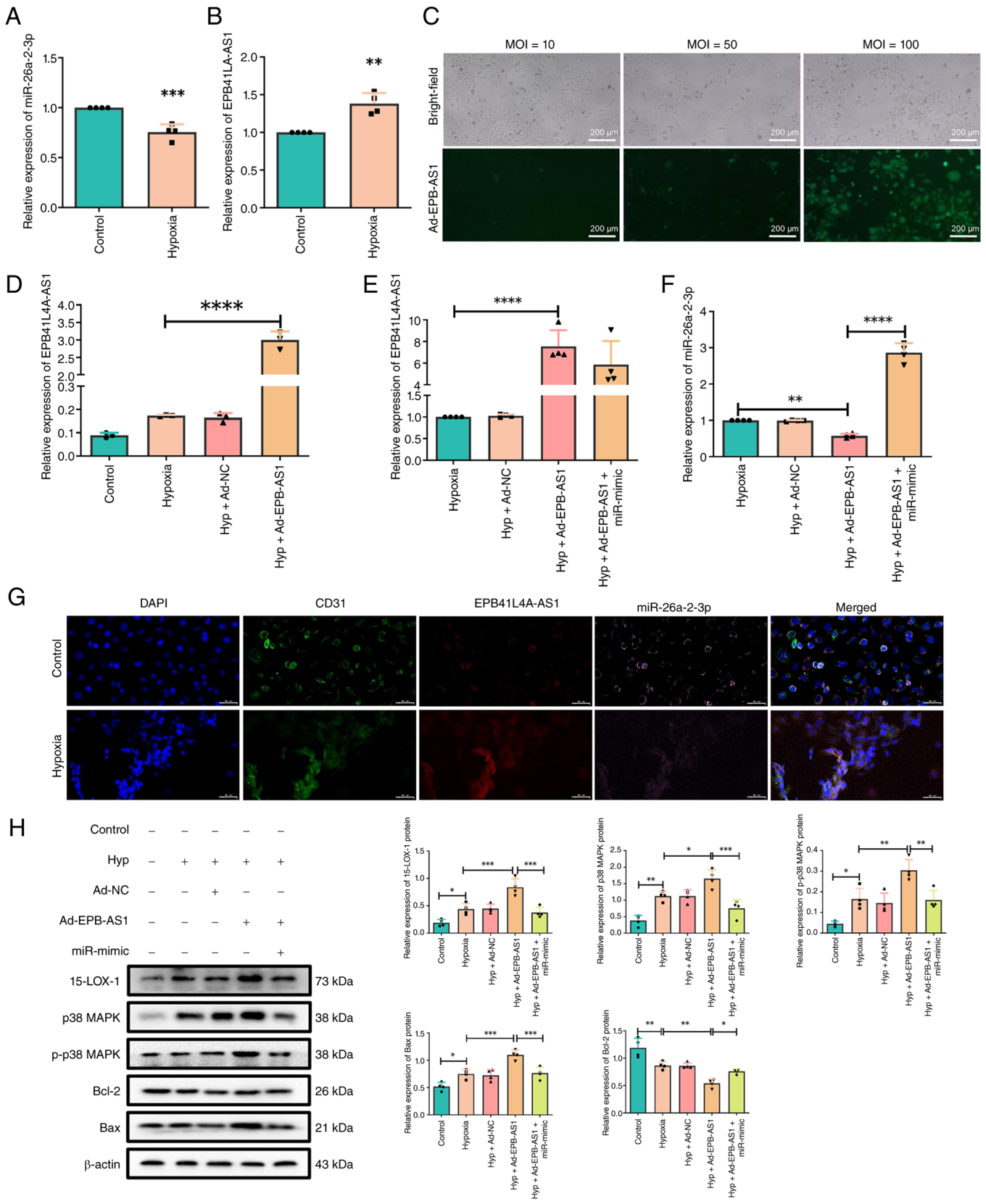


Figure 2. EPB41L4A-AS1 regulates miR-26a-2-3p/15-LOX-1/p38 MAPK axis in HUVECs. (A and B) The expression of EPB41L4A-AS1 and miR-26a-2-3p of HUVECs treated with hypoxia (n=4). (C and D) Screening of MOI values for EPB41L4A-AS1 overexpression adenovirus. EPB41L4A-AS1 overexpressing adenovirus (green). MOI=10, 50, 100. Scale bars, 200 μm. (E and F) Effect of EPB41L4A-AS1 overexpression and miR-26a-2-3p mimic intervention on the expression of EPB41L4A-AS1 and miR-26a-2-3p in HUVECs treated with hypoxia (n=4). (G) The colocalization of EPB41L4A-AS1 and miR-26a-2-3p in HUVECs by the method of immunofluorescence and fluorescence *in situ* hybridization assays. EPB41L4A-AS1 (red), DAPI (blue), miR-26a-2-3p (pink), CD31 (green), scale bars, 50 μm. (H) Effect of EPB41L4A-AS1 overexpression and miR-26a-2-3p mimic intervention on the expression of 15-LOX-1, p38 MAPK, phospho-p38 MAPK, Bax, and Bcl-2 protein in hypoxia HUVECs (n=4). *P<0.05, **P<0.01, ***P<0.001 and ****P<0.0001. Hyp, hypoxia; Ad-NC, non-coding adenovirus; Ad-EPB-AS1, adenovirus overexpressing EPB41L4A-AS1; MOI, multiplicity of infection; 15-LOX-1, 15-lipoxygenase-1.

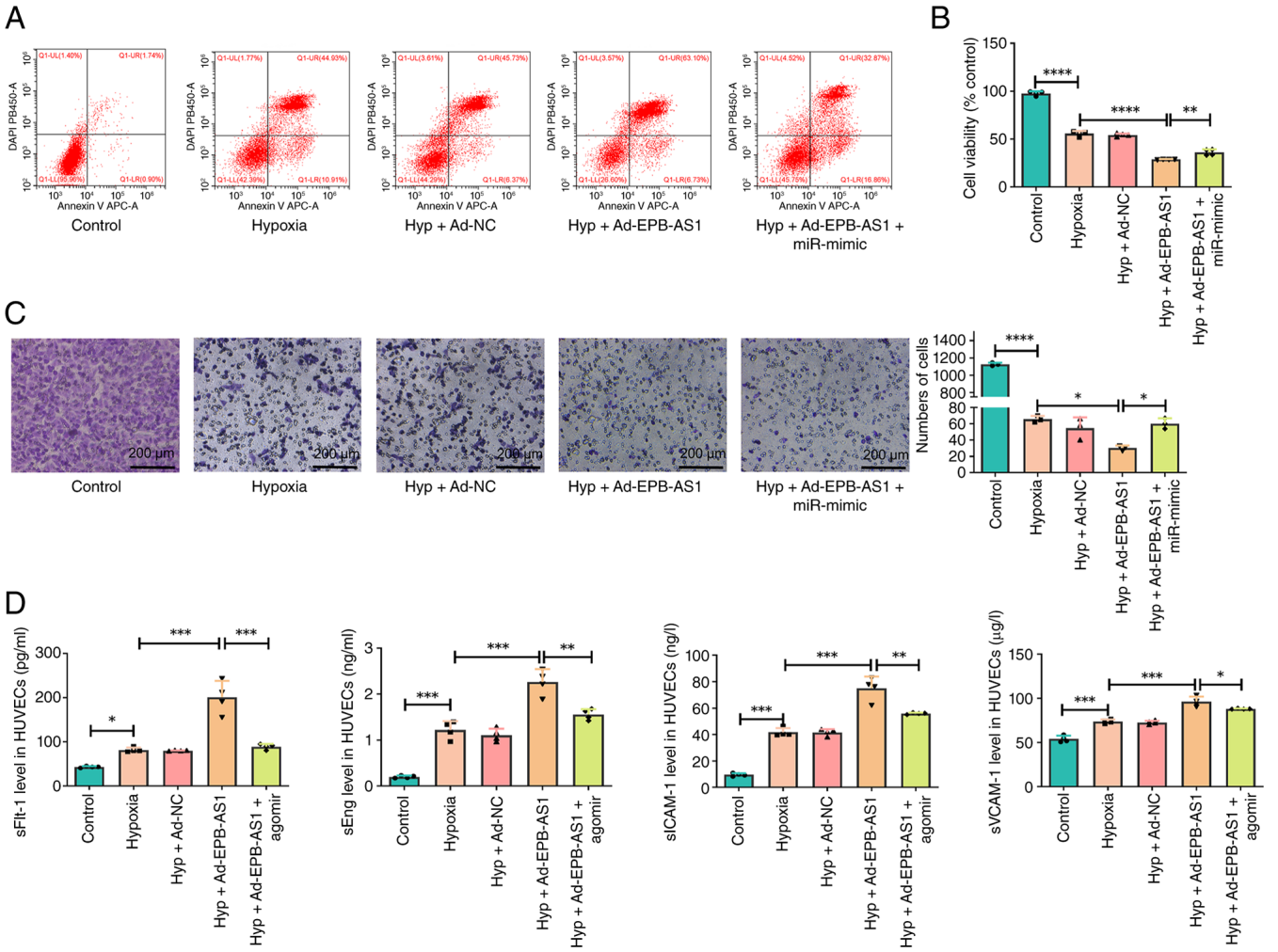


Figure 3. EPB41L4A-AS1 promoted the endothelial cells injury induced by hypoxia through miR-26a-2-3p/15-LOX-1/p38 MAPK axis in HUVECs. (A) Effect of EPB41L4A-AS1 overexpression and miR-26a-2-3p mimic intervention on apoptosis of HUVECs caused by hypoxia. (B) Effect of EPB41L4A-AS1 overexpression and miR-26a-2-3p mimic intervention on cell viability in hypoxia-treated HUVECs (n=4). (C) Effect of EPB41L4A-AS1 overexpression and miR-26a-2-3p mimic intervention on migration of HUVECs caused by hypoxia. Scale bars, 200 μm (n=4). (D) Effect of EPB41L4A-AS1 overexpression and miR-26a-2-3p mimic intervention on the content of sENG, sFlt-1, sICAM-1 and sVCAM-1 in hypoxia-treated HUVECs (n=4). *P<0.05, **P<0.01, ***P<0.001 and ****P<0.0001. Hyp, hypoxia; Ad-NC, non-coding adenovirus; Ad-EPB-AS1, adenovirus overexpressing EPB41L4A-AS1.

therapeutic options for PE remain limited, with induced delivery serving as the definitive intervention to prevent disease progression (31). Consequently, elucidating the pathogenesis of PE and discovering novel therapeutic targets are critical for improving clinical outcomes. Accumulating studies indicate that multiple lncRNAs serve as critical players in the development and progression of PE (32,33). For example, elevated circulating levels of lncRNA BC030099 have been reported to be associated with elevated PE risk, highlighting its potential as a diagnostic biomarker (34). Jiang *et al* (35) reported that dysregulation of the 'INHBA-AS1-CENPB-TRAF1' pathway was a contributor to the pathogenesis of PE through prohibiting the proliferation, invasion and migration of trophoblasts during placentation. Emerging evidence indicates that EPB41L4A-AS1 contributes to the pathogenesis of early recurrent miscarriage through its regulatory effects on trophoblast metabolic processes. Furthermore, its expression is elevated in various pregnancy-related pathologies, including intrauterine growth restriction, miscarriage and PE (26). The present investigation identified a significant upregulation of EPB41L4A-AS1 in placental specimens obtained from patients with PE; therefore, it is hypothesized that EPB41L4A-AS1 may assume a central pathological role in the development of PE.

Maternal systemic endothelial dysfunction represents a fundamental aspect of the pathological mechanisms underlying PE (12). This dysfunction is characterized by an increase in inflammatory cytokines and oxidative stress, apoptosis of endothelial cells and impaired endothelial cell proliferation and migration (36-38). Through comprehensive investigation, the present study established the modulatory influence of EPB41L4A-AS1 on multiple aspects of endothelial cell biology. The present current findings demonstrate that EPB41L4A-AS1 upregulation significantly suppressed endothelial cell proliferation, impaired migratory capacity and enhanced apoptotic activity. Increased concentrations of VCAM-1 and ICAM-1 represent well-established markers of endothelial inflammation, while sFlt-1 and sENG are recognized as key antiangiogenic mediators in the pathogenesis of PE (39,40). Under hypoxic conditions, EPB41L4A-AS1 overexpression notably elevated the expression of key pathogenic factors

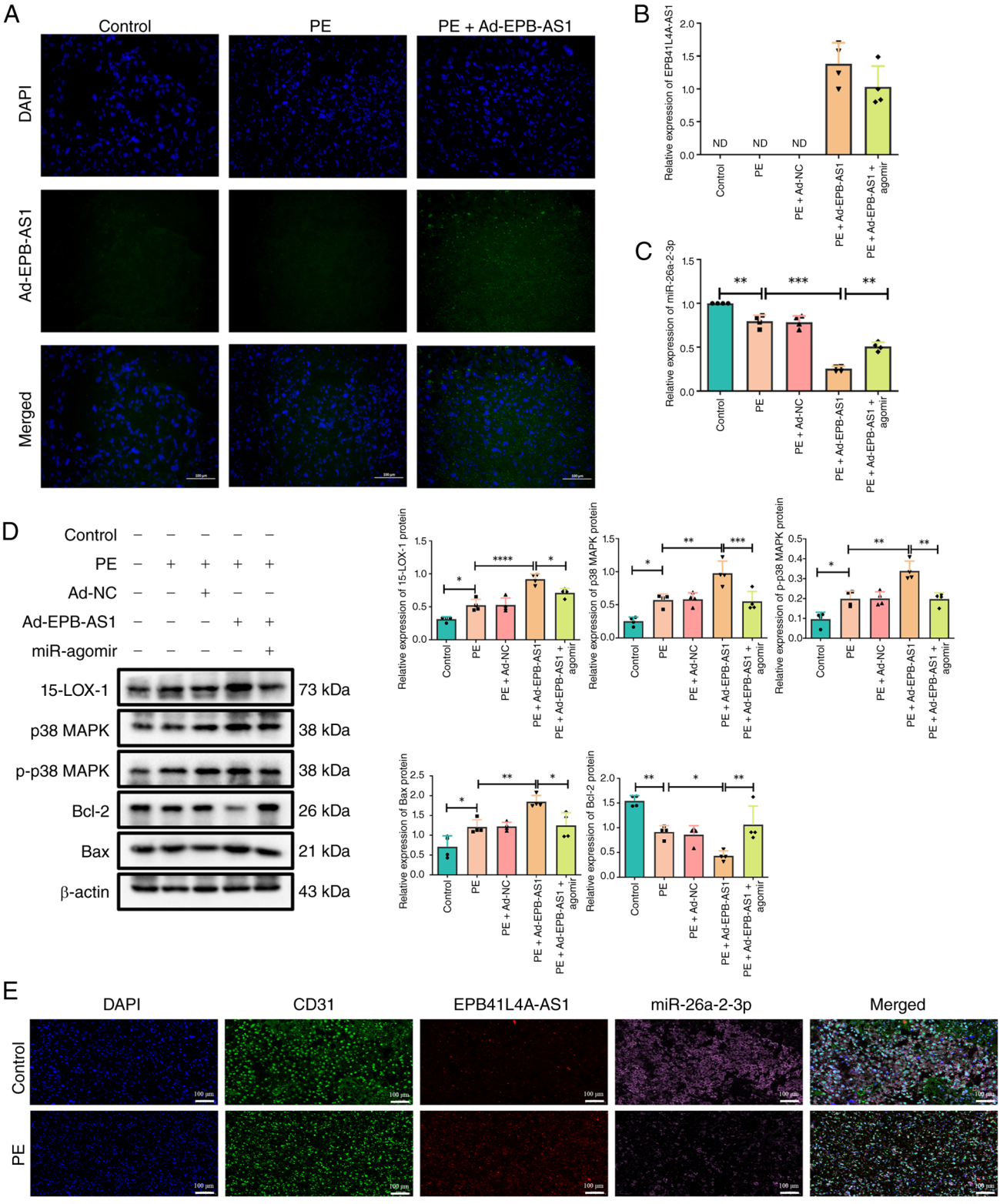


Figure 4. EPB41L4A-AS1 regulates miR-26a-2-3p/15-LOX-1/p38 MAPK axis *in vivo*. (A) Mouse placenta was successfully infected by EPB41L4A-AS1 overexpressed adenovirus. Frozen sections of mouse placenta, DAPI (blue), EPB41L4A-AS1 (green), scale bars, 100 μm. (B and C) The expression of EPB41L4A-AS1 and miR-26a-2-3p in the placentas of PE-like mice following the overexpression of EPB41L4A-AS1 and miR-26a-2-3p agomir intervention. (D) Effect of EPB41L4A-AS1 overexpression and miR-26a-2-3p agomir intervention on 15-LOX-1, p38 MAPK, phospho-p38 MAPK, Bax and Bcl-2 protein expression in preeclamptic mice (n=4). *P<0.05, **P<0.01, ***P<0.001 and ****P<0.0001. (E) The colocalization of EPB41L4A-AS1 and miR-26a-2-3p in mouse placenta by the method of immunofluorescence and fluorescence *in situ* hybridization assays. EPB41L4A-AS1 (red), DAPI (blue), miR-26a-2-3p (pink), CD31 (green), scale bars, 100 μm. PE, preeclampsia; 15-LOX-1, 15-lipoxygenase-1; Ad-NC, non-coding adenovirus; Ad-EPB-AS1, adenovirus overexpressing EPB41L4A-AS1; ND, not detected.

including sVCAM-1, sICAM-1, sFlt-1 and sENG in endothelial cells. The functional connection between EPB41L4A-AS1 and endothelial impairment was further validated in the PE mouse model. Adenovirus-mediated EPB41L4A-AS1 overexpression

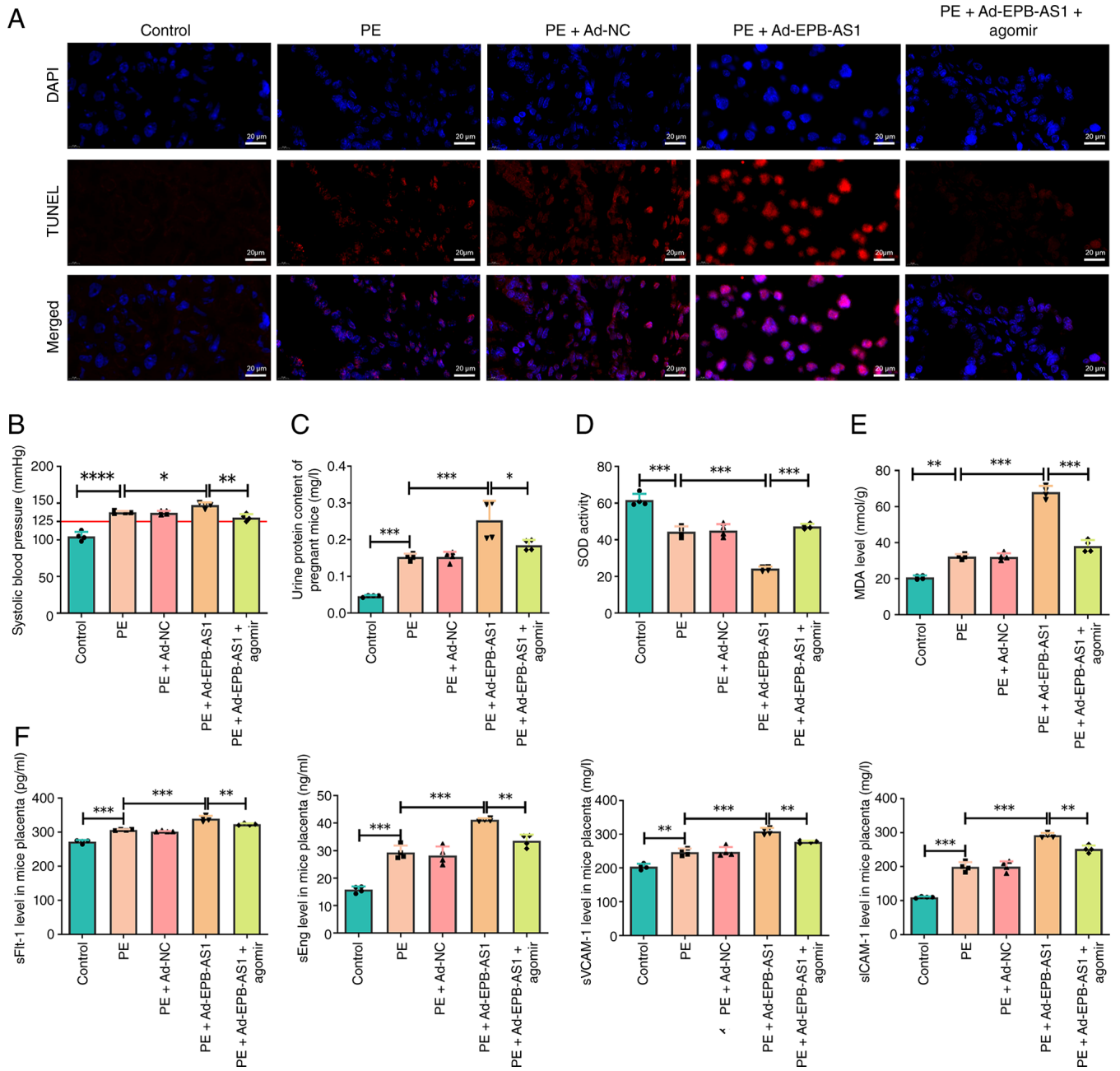


Figure 5. EPB41L4A-AS1 activated 15-LOX-1/p38 MAPK axis to promote endothelial cell injury via mediating miR-26a-2-3p in PE-like mice. (A) Effect of EPB41L4A-AS1 overexpression and miR-26a-2-3p agomir on placental cell apoptosis in mice with preeclampsia. TUNEL (red), DAPI (blue). Scale bars, 20 μm. (B) Changes in systolic blood pressure in pregnant mice (n=4). (C) Changes in urinary proteins in pregnant mice. (n=4). (D and E) Effects of EPB41L4A-AS1 overexpression and miR-26a-2-3p agomir on SOD activity and MDA levels in placenta of preeclampsia mice (n=4). (F) Effect of EPB41L4A-AS1 overexpression and miR-26a-2-3p agomir on the placental tissue of preeclamptic mice with sENG, sFlt-1, sICAM-1 and sVCAM-1 content (n=4). *P<0.05, **P<0.01, ***P<0.001 and ****P<0.0001. PE, preeclampsia; 15-LOX-1, 15-lipoxygenase-1; Ad-NC, non-coding adenovirus; Ad-EPB-AS1, adenovirus overexpressing EPB41L4A-AS1.

induced a coordinated upregulation of sVCAM-1, sICAM-1, sFlt-1 and sENG in placental tissues, while also exacerbating apoptotic responses. Patients with PE exhibit compromised placental antioxidant defense, characterized by reduced expression of SOD and glutathione peroxidase compared with normotensive pregnancies (7). Notably, the present study found that EPB41L4A-AS1 significantly decreased SOD activity and increased MDA content in mouse placenta. These collective results underscore the detrimental role of EPB41L4A-AS1 in fostering endothelial dysfunction through impairing cell viability and migration and angiogenesis while intensifying apoptosis, oxidative stress injury and inflammatory cell adhesion. Consequently, therapeutic targeting of EPB41L4A-AS1 and its downstream pathways represents a novel therapeutic approach for alleviating PE-associated vascular dysfunction.

Numerous studies indicate that lncRNAs frequently function as molecular sponges for miRNAs, thereby implementing post-transcriptional regulation (24,41,42). For example, in preeclamptic placentas, KCNQ1OT1 expression was markedly downregulated and functional studies

demonstrated that silencing this lncRNA in trophoblasts compromised cellular invasion through its interaction with miR-146a-3p (43). Fan *et al* (44) reported that suppression of NEAT1 upregulates miR-411-5p and inhibits PTEN, thereby stimulating trophoblast behaviors critical for placental development and counteracting PE progression. In the present study, bioinformatic analysis suggested a potential binding capacity between EPB41L4A-AS1 and miR-26a-2-3p, as complementary sequences were identified. Therefore, the present study subsequently investigated the potential roles and relationships of EPB41L4A-AS1 and miR-26a-2-3p in PE. Cellular co-localization of EPB41L4A-AS1 and miR-26a-2-3p was confirmed, with expression profiling demonstrating a reciprocal relationship that may hold pathophysiological significance. EPB41L4A-AS1 overexpression downregulated miR-26a-2-3p expression in hypoxic endothelial cells, which was further validated in placental tissues from PE-like mice. Both *in vivo* and *in vitro* functional studies demonstrate that elevating miR-26a-2-3p levels rescues the detrimental effects of EPB41L4A-AS1 on endothelial function. In addition, the therapeutic elevation of miR-26a-2-3p ameliorated the EPB41L4A-AS1-induced hypertension and proteinuria in the PE mouse model. Our earlier work established that miR-26a-2-3p directly targets 15-LOX-1, leading to suppressed p38 MAPK pathway activation and consequent attenuation of endothelial impairment in PE (23). The current investigation identified a marked upregulation of EPB41L4A-AS1 in preeclamptic placentas, which mediated a concomitant suppression of miR-26a-2-3p. This suppression subsequently triggered activation of the 15-LOX-1/p38 MAPK signaling axis, culminating in endothelial dysfunction.

An increasing body of evidence indicates that lncRNA regulates cell phenotypes by influencing gene expression through multiple mechanisms (45-47). A previous study demonstrates that EPB41L4A-AS1 interacts with SET1A, thereby increasing the H3K4me3 level at the VDAC1 promoter and regulating VDAC1 expression (26). Concurrently, research reveals that SETD2-mediated H3K36me3 histone modification affects m6A RNA methylation (48), and m6A modification can influence miRNA processing, stability and function (49). Methylation modifications have been detected in a large proportion of human miRNAs (50), suggesting that miRNA methylation is a widespread regulatory mechanism. As members of the miR-26 family, miR-26a-2-3p and miR-26-5p share a conserved seed sequence and exhibit high evolutionary conservation. Notably, a specific methylation motif has been identified in miR-26-5p (51), raising the possibility that analogous methylation-based regulation may also apply to miR-26a-2-3p. Because the dual-luciferase assay excluded direct binding between EPB41L4A-AS1 and miR-26a-2-3p, we hypothesize that EPB41L4A-AS1 may indirectly suppress miR-26a-2-3p by altering histone methylation and downstream m6A-dependent processing of its primary transcript, thereby contributing to PE pathogenesis. This model requires further experimental validation.

Several limitations should be acknowledged when interpreting the findings of the present study. First, the clinical sample size was relatively modest; although statistically significant differences were observed, larger multicenter cohorts are needed to confirm the present results. Second, while the L-NAME induced PE mouse model mimics certain clinical features such as hypertension and proteinuria, it does not fully recapitulate the complex pathophysiology of human PE, particularly regarding placental development, immune adaptation and systemic vascular responses. Thus, caution is warranted when extrapolating findings from this model to human disease. Third, the present investigation focused primarily on EPB41L4A-AS1 expression in placental tissues and its functional role in endothelial cells. The expression patterns and functional relevance of this lncRNA in other maternal tissues, including systemic vascular endothelium, kidney and liver, remain to be explored. Given the multisystem nature of PE, the potential involvement of EPB41L4A-AS1 in these organs warrants further investigation. Collectively, future studies involving expanded clinical cohorts, improved animal models that more closely reflect human PE and comprehensive evaluation of EPB41L4A-AS1 function across multiple organ systems are necessary to fully elucidate its role in the pathogenesis of PE.

Acknowledgements

Not applicable.

Funding

The present study was funded by the National Natural Science Foundation of China (grant no. 82574487).

Availability of data and materials

The data generated in the present study may be requested from the corresponding author.

Authors' contributions

JH conceived and designed the study, conducted the investigation, curated and formally analyzed the data and drafted the original manuscript. HR conceived and designed the study, conducted the investigation, curated the data, drafted the original manuscript and critically revised the manuscript. RX and XC conducted the investigation, curated the data and performed formal analysis. ZP, YL and YZ conducted the investigation, provided resources, recruited patients and collected clinical data. DR conducted the investigation, interpreted the data and critically revised the manuscript. LC conceived and supervised the study, curated the data, acquired funding and critically revised the manuscript. JY conceived and supervised the study, curated the data, administered the project, drafted the original manuscript, and critically revised the manuscript. LC and JY confirm the authenticity of all raw data. All authors read and approved the final version of the manuscript.

Ethics approval and consent to participate

The study received formal approval from the institutional ethics board (SYXK YU 20220016, no. 2022033) at the Women and Children's Hospital of Chongqing Medical University. Documented consent was acquired from all participating individuals. All animal experimental procedures

were in compliance with the Ethical Committee for Animal Experimentation at Chongqing Medical University (approval no. SYXK-2022-0016).

Patient consent for publication

Not applicable.

Competing interests

The authors declare no competing interests.

References

1. Mol BWJ, Roberts CT, Thangaratinam S, Magee LA, de Groot CJM and Hofmeyr GJ: Pre-eclampsia. Lancet 387: 999-1011, 2016.
2. No authors listed: Gestational hypertension and preeclampsia: ACOG practice bulletin, number 222. Obstet Gynecol 135: e237-e260, 2020.
3. Fantone S, Ermini L, Piani F, Di Simone N, Barbaro G, Giannubilo SR, Gesuita R, Tossetta G and Marzioni D: Downregulation of argininosuccinate synthase 1 (ASS1) is associated with hypoxia in placental development. Hum Cell 36: 1190-1198, 2023.
4. Marzioni D, Piani F, Di Simone N, Giannubilo SR, Ciavattini A and Tossetta G: Importance of STAT3 signaling in preeclampsia (Review). Int J Mol Med 55: 58, 2025.
5. Tossetta G, Campagna R, Fantone S, Di Simone N, Pompei V, Giannubilo SR, Ciavattini A, Sartini D, Emanuelli M and Marzioni D: NNMT expression in preeclampsia: Analyses on placental tissues and cell lines. Placenta 171: 111-120, 2025.
6. Magee LA, Nicolaides KH and von Dadelszen P: Preeclampsia. N Engl J Med 386: 1817-1832, 2022.
7. Rana S, Lemoine E, Granger JP and Karumanchi SA: Preeclampsia: Pathophysiology, challenges, and perspectives. Circ Res 124: 1094-1112, 2019.
8. Ala U: Competing endogenous RNAs, non-coding RNAs and diseases: An intertwined story. Cells 9: 1574, 2020.
9. Kornacki J, Olejniczak O, Sibiak R, Gutaj P and Wender-Ożegowska E: Pathophysiology of pre-eclampsia-two theories of the development of the disease. Int J Mol Sci 25: 307, 2023.
10. Redman CWG, Staff AC and Roberts JM: Syncytiotrophoblast stress in preeclampsia: The convergence point for multiple pathways. Am J Obstet Gynecol 226: S907-S927, 2022.
11. Staff AC, Fjeldstad HE, Fosheim IK, Moe K, Turowski G, Johnsen GM, Alnaes-Katjavivi P and Sugulle M: Failure of physiological transformation and spiral artery atherosis: Their roles in preeclampsia. Am J Obstet Gynecol 226: S895-S906, 2022.
12. Poon LC, Shennan A, Hyett JA, Kapur A, Hadar E, Divakar H, McAuliffe F, da Silva Costa F, von Dadelszen P, McIntyre HD, *et al*: The international federation of gynecology and obstetrics (FIGO) initiative on pre-eclampsia: A pragmatic guide for first-trimester screening and prevention. Int J Gynaecol Obstet 145 (Suppl 1): S1-S33, 2019.
13. Guay C and Regazzi R: Circulating microRNAs as novel biomarkers for diabetes mellitus. Nat Rev Endocrinol 9: 513-521, 2013.
14. Jiménez-Lucena R, Camargo A, Alcalá-Diaz JF, Romero-Baldonado C, Luque RM, van Ommen B, Delgado-Lista J, Ordovás JM, Pérez-Martínez P, Rangel-Zúñiga OA and López-Miranda J: A plasma circulating miRNAs profile predicts type 2 diabetes mellitus and prediabetes: From the CORDIOPREV study. Exp Mol Med 50: 1-12, 2018.
15. Lu TX and Rothenberg ME: MicroRNA. J Allergy Clin Immunol 141: 1202-1207, 2018.
16. Aplin JD, Myers JE, Timms K and Westwood M: Tracking placental development in health and disease. Nat Rev Endocrinol 16: 479-494, 2020.
17. Chen DB and Wang W: Human placental microRNAs and preeclampsia. Biol Reprod 88: 130, 2013.
18. Brodowski L, Schröder-Heurich B, von Hardenberg S, Richter K, von Kaisenberg CS, Dittrich-Breiholz O, Meyer N, Dörk T and von Versen-Höynck F: MicroRNA profiles of maternal and neonatal endothelial progenitor cells in preeclampsia. Int J Mol Sci 22: 5320, 2021.
19. Kim S, Lee KS, Choi S, Kim J, Lee DK, Park M, Park W, Kim TH, Hwang JY, Won MH, *et al*: NF-κB-responsive miRNA-31-5p elicits endothelial dysfunction associated with preeclampsia via down-regulation of endothelial nitric-oxide synthase. J Biol Chem 293: 18989-19000, 2018.
20. Kim S, Park M, Kim JY, Kim T, Hwang JY, Ha KS, Won MH, Ryoo S, Kwon YG and Kim YM: Circulating miRNAs associated with dysregulated vascular and trophoblast function as target-based diagnostic biomarkers for preeclampsia. Cells 9: 2003, 2020.
21. Kim S, Shim S, Kwon J, Ryoo S, Byeon J, Hong J, Lee JH, Kwon YG, Kim JY and Kim YM: Alleviation of preeclampsia-like symptoms through PlGF and eNOS regulation by hypoxia- and NF-κB-responsive miR-214-3p deletion. Exp Mol Med 56: 1388-1400, 2024.
22. Zhou C, Zou QY, Li H, Wang RF, Liu AX, Magness RR and Zheng J: Preeclampsia downregulates MicroRNAs in fetal endothelial cells: Roles of miR-29a/c-3p in endothelial function. J Clin Endocrinol Metab 102: 3470-3479, 2017.
23. Chen L, Peng Z, Yang Y, He J, Lv Z, Zheng Q, Lei T, Guo W, Chen Z, Liu Y, *et al*: The neo-potential therapeutic strategy in preeclampsia: Downregulated miR-26a-2-3p motivates endothelial cell injury by targeting 15-LOX-1. Free Radic Biol Med 225: 112-126, 2024.
24. Chan JJ and Tay Y: Noncoding RNA:RNA regulatory networks in cancer. Int J Mol Sci 19: 1310, 2018.
25. Hu X, Ao J, Li X, Zhang H, Wu J and Cheng W: Competing endogenous RNA expression profiling in pre-eclampsia identifies hsa_circ_0036877 as a potential novel blood biomarker for early pre-eclampsia. Clin Epigenetics 10: 48, 2018.
26. Zhu Y, Liu Q, Liao M, Diao L, Wu T, Liao W, Wang Z, Li B, Zhang S, Wang S, *et al*: Overexpression of lncRNA EPB41L4A-AS1 induces metabolic reprogramming in trophoblast cells and placenta tissue of miscarriage. Mol Ther Nucleic Acids 36: 102411, 2024.
27. Hussey MR, MacDonald J, Bammler TK, Tekola-Ayele F, Kerr KF, Paquette AG, Marsit CJ, LeWinn KZ, Zhao Q, Karr CJ, *et al*: Associations of placental lncRNA expression with maternal pre-pregnancy BMI and infant birthweight in two birth cohorts. J Dev Orig Health Dis 16: e20, 2025.
28. Cunningham FG, Leveno KJ, Bloom SL, Spong CY, Dashe JS, Hoffman BL, Casey BM and Sheffield JS: Williams obstetrics. 24th edition. McGraw-Hill Education/Medical, New York, NY, 2014.
29. Amaral TAS, Ognibene DT, Carvalho LCRM, Rocha APM, Costa CA, Moura RS and Resende AC: Differential responses of mesenteric arterial bed to vasoactive substances in L-NAME-induced preeclampsia: Role of oxidative stress and endothelial dysfunction. Clin Exp Hypertens 40: 126-135, 2018.
30. Livak KJ and Schmittgen TD: Analysis of relative gene expression data using real-time quantitative PCR and the 2(-Delta Delta C(T)) method. Methods 25: 402-408, 2001.
31. Phipps EA, Thadhani R, Benzing T and Karumanchi SA: Pre-eclampsia: Pathogenesis, novel diagnostics and therapies. Nat Rev Nephrol 15: 275-289, 2019.
32. Chiang YT, Seow KM and Chen KH: The pathophysiological, genetic, and hormonal changes in preeclampsia: A systematic review of the molecular mechanisms. Int J Mol Sci 25: 4532, 2024.
33. Sun N, Qin S, Zhang L and Liu S: Roles of noncoding RNAs in preeclampsia. Reprod Biol Endocrinol 19: 100, 2021.
34. Sun Y, Hou Y, Lv N, Liu Q, Lin N, Zhao S, Chu X, Chen X, Cheng G, Li P *et al*: Circulating lncRNA BC030099 increases in preeclampsia patients. Mol Ther Nucleic Acids 14: 562-566, 2019.
35. Jiang S, Chen Q, Liu H, Gao Y, Yang X, Ren Z, Gao Y, Xiao L, Zhong M, Yu Y and Yang X: Preeclampsia-associated lncRNA INHBA-AS1 regulates the proliferation, invasion, and migration of placental trophoblast cells. Mol Ther Nucleic Acids 22: 684-695, 2020.
36. Degner K, Magness RR and Shah DM: Establishment of the human uteroplacental circulation: A historical perspective. Reprod Sci 24: 753-761, 2017.
37. Nourollahpour Shiadeh M, Behboodi Moghadam Z, Adam I, Saber V, Bagheri M and Rostami A: Human infectious diseases and risk of preeclampsia: An updated review of the literature. Infection 45: 589-600, 2017.
38. Wang Y, Gu Y, Zhang Y and Lewis DF: Evidence of endothelial dysfunction in preeclampsia: Decreased endothelial nitric oxide synthase expression is associated with increased cell permeability in endothelial cells from preeclampsia. Am J Obstet Gynecol 190: 817-824, 2004.

39. Higgins JR, Papayianni A, Brady HR, Darling MR and Walshe JJ: Circulating vascular cell adhesion molecule-1 in pre-eclampsia, gestational hypertension, and normal pregnancy: Evidence of selective dysregulation of vascular cell adhesion molecule-1 homeostasis in pre-eclampsia. Am J Obstet Gynecol 179: 464-469, 1998.
40. Torres-Torres J, Espino-Y-Sosa S, Martinez-Portilla R, Borboa-Olivares H, Estrada-Gutierrez G, Acevedo-Gallegos S, Ruiz-Ramirez E, Velasco-Espin M, Cerda-Flores P, Ramirez-Gonzalez A and Rojas-Zepeda L: A narrative review on the pathophysiology of preeclampsia. Int J Mol Sci 25: 7569, 2024.
41. Wei X, Yuan Y and Yang Q: SNHG22 promotes migration and invasion of trophoblasts via miR-128-3p/PCDH11X axis and activates PI3K/Akt signaling pathway. Clinics (Sao Paulo) 77: 100055, 2022.
42. Roberts JM and Hubel CA: Is oxidative stress the link in the two-stage model of pre-eclampsia? Lancet 354: 788-789, 1999.
43. Chen FR, Zheng LM, Wu DC, Gong HM, Cen H and Chen WC: Regulatory relationship between lncRNA KCNQ1OT1 and miR-146a-3p in preeclampsia. Zhonghua Fu Chan Ke Za Zhi 55: 535-543, 2020 (In Chinese).
44. Fan X, Lou J, Zheng X, Wang Y, Wang J, Luo M and Hu M: Interference with lncRNA NEAT1 promotes the proliferation, migration, and invasion of trophoblasts by upregulating miR-411-5p and inhibiting PTEN expression. Immunopharmacol Immunotoxicol 43: 334-342, 2021.
45. Arvaniti E, Moulos P, Vakrakou A, Chatziantoniou C, Chadjichristos C, Kavvadas P, Charonis A and Politis PK: Whole-transcriptome analysis of UUO mouse model of renal fibrosis reveals new molecular players in kidney diseases. Sci Rep 6: 26235, 2016.
46. Peng WX, Koirala P and Mo YY: LncRNA-mediated regulation of cell signaling in cancer. Oncogene 36: 5661-5667, 2017.
47. Yu D, Zhao Z, Wang L, Qiao S, Yang Z, Wen Q and Zhu G: SOX21-AS1 activated by STAT6 promotes pancreatic cancer progression via up-regulation of SOX21. J Transl Med 20: 511, 2022.
48. Huang H, Weng H, Zhou K, Wu T, Zhao BS, Sun M, Chen Z, Deng X, Xiao G, Auer F, *et al*: Histone H3 trimethylation at lysine 36 guides m^6A RNA modification co-transcriptionally. Nature 567: 414-419, 2019.
49. Su N, Yu X, Duan M and Shi N: Recent advances in methylation modifications of microRNA. Genes Dis 12: 101201, 2023.
50. Yang R, Li J, Wu Y, Jiang X, Qu S, Wang Q, Liang H and Zen K: A novel method to purify small RNAs from human tissues for methylation analysis by LC-MS/MS. Front Mol Biosci 9: 949181, 2022.
51. Li C, Li Y, Lu Y, Niu Z, Zhao H, Peng Y and Li M: miR-26 family and its target genes in tumorigenesis and development. Crit Rev Oncol Hematol 157: 103124, 2021.

Copyright © 2026 He et al. This work is licensed under a Creative Commons Attribution-NonCommercial-NoDerivatives 4.0 International (CC BY-NC-ND 4.0) License.